

Alix regulates cortical actin and the spatial distribution of endosomes

Alicia Cabezas, Kristi G. Bache, Andreas Brech and Harald Stenmark*

Department of Biochemistry, the Norwegian Radium Hospital, Montebello, 0310 Oslo, Norway

*Author for correspondence (e-mail: stenmark@ulrik.uio.no)

Accepted 16 March 2005

Journal of Cell Science 118, 2625-2635 Published by The Company of Biologists 2005
doi:10.1242/jcs.02382

Summary

Alix/AIP1 is a proline-rich protein that has been implicated in apoptosis, endocytic membrane trafficking and viral budding. To further elucidate the functions of Alix, we used RNA interference to specifically suppress its expression. Depletion of Alix caused a striking redistribution of early endosomes from a peripheral to a perinuclear location. The redistribution of endosomes did not affect transferrin recycling or degradation of endocytosed epidermal growth factor receptors, although the uptake of transferrin was mildly reduced when Alix was downregulated. Quantitative immunoelectron microscopy showed that multivesicular endosomes of Alix-depleted cells contained normal amounts of CD63, whereas their levels of lyso-

bisphosphatidic acid were reduced. Alix depletion also caused an accumulation of unusual actin structures that contained clathrin and cortactin, a protein that couples membrane dynamics to the cortical actin cytoskeleton. Our results suggest that Alix functions in the actin-dependent intracellular positioning of endosomes, but that it is not essential for endocytic recycling or for trafficking of membrane proteins between early and late endosomes in non-polarised cells.

Key words: Alix, Membrane traffic, Actin, Cortactin, Clathrin, Hip1R

Introduction

Endocytosis is essential for constitutive uptake of protein-bound nutrients and for ligand-induced receptor downregulation. Internalised molecules are delivered to early endosomes, where activated growth factor receptors are sorted into late endosomes and lysosomes for degradation while nutrient receptors are recycled to the plasma membrane (Gruenberg, 2001). The molecular machineries that mediate endocytosis and endosomal sorting are currently being characterized; here we have studied the functions of a protein that has been implicated in the regulation of protein trafficking through endosomes.

Alix, also known as AIP1, was first identified as an ALG-2 (apoptosis-linked gene 2)-interacting protein (Missotten et al., 1999; Vito et al., 1999). Recent data have shown a connection between Alix and the multivesicular body (MVB) pathway and viral budding. MVBs mediate the transport between early endosomes and late endosomes/lysosomes. This pathway is required for a number of biological processes, such as growth factor receptor downregulation, antigen presentation and retroviral budding. Mono- and multi-ubiquitination function as signals for endocytic membrane cargo to enter the MVB pathway (Haglund et al., 2003). The machinery that sorts ubiquitinated cargo into MVBs has been partially characterised (Raiborg et al., 2003). Hrs (hepatocyte growth factor-regulated tyrosine kinase substrate), a phosphoinositide- and ubiquitin-binding protein, is a key component of this machinery (Raiborg et al., 2002). It is thought to interact with ubiquitinated membrane proteins and to deliver these further to the so-called endosomal sorting complexes required for transport (ESCRTs)

(Bache et al., 2003; Katzmann et al., 2003). The three ESCRTs are recruited consecutively to the limiting membrane of endosomes to sort ubiquitinated cargo and to initiate invagination and vesiculation of the endosome membrane (Katzmann et al., 2002).

Human immunodeficiency virus (HIV), equine infectious anaemia virus (EIAV) and other retroviruses exit infected cells by budding from the plasma membrane, a process that requires membrane fission. The late domain of HIV-1 Gag mediates the detachment of the virion by recruiting ESCRT-I (Amara and Littman, 2003). Alix has been shown to interact with the Tsg101 and CHMP4 components of the ESCRT-I and III complexes, respectively, and with the HIV-1 Gag and EIAV-Gag proteins (Kato et al., 2004; Strack et al., 2003; von Schwedler et al., 2003). In addition, Alix associates with lyso-bisphosphatidic acid (LBPA)-containing liposomes. LBPA is a structural isomer of phosphatidylglycerol that is highly enriched in internal membranes of late endosomes (Kobayashi et al., 1998), and may regulate the dynamics and functions of the internal membranes inside the MVBs and late endosomes (Dikic, 2004; Matsuo et al., 2004).

Alix also binds endophilins, which are thought to regulate membrane shape during endocytosis (Chatellard-Causse et al., 2002), and CIN85/SETA (Borinstein et al., 2000; Chen et al., 2000), which is involved in signal transduction and endocytosis of ubiquitinated tyrosine kinase receptors. Moreover, Alix has been reported to associate with structural proteins of the cytoskeleton, including actin and tubulins, and both CIN85 and Alix interact with focal adhesion kinase (FAK) and proline rich tyrosine kinase 2 (PYK-2) (Schmidt et al., 2003).

Even though Alix has been implicated in a number of cellular processes, its precise functions are not known. In the present work, we have used small interfering RNA (siRNA) to suppress the expression of Alix. We show herein that Alix is needed to maintain the proper cellular distribution of endosomes, but that it is not rate-limiting for receptor sorting, recycling or degradation. Importantly, downregulation of Alix produces an effect on actin organisation that is reminiscent of that previously found with downregulation of Hip1R, a protein thought to facilitate the transient interaction between actin and the endocytic machinery. These results suggest a role for Alix in the connection between the cortical actin cytoskeleton and endosomes.

Materials and Methods

Design of siRNA duplexes

RNAs (21 nucleotides in length) were chemically synthesised and gel-purified (Eurogentec, Seraing, Belgium), and the siRNA duplexes were prepared as described by the manufacturer. For RNA interference against Alix, we used oligonucleotides with sense sequence 5'-GCCGCGUGAAGUUCAUUCTT-3' and antisense sequence 5'-GAUGAACUUCACCAGCGGCTT-3', corresponding to nucleotides 57-75 in Alix. A BLAST search confirmed that this sequence was unique to Alix. As negative control, we used scrambled sequences of the same nucleotides: sense control 5'-ACUUCGAGCGUGCAUGGCUTT-3' and anti-sense control 5'-AGCC-AUGCACGCUCGAAGUTT-3'.

Cell culture siRNA treatment

HeLa cell cultures were maintained in DMEM with 2 mM L-glutamine, supplemented with 10% foetal calf serum (FCS), 100 U/ml penicillin and 100 µg/ml streptomycin at 37°C in a humidified atmosphere with 5% CO₂. Transfections of HeLa cells with siRNA against Alix were performed as described (Elbashir et al., 2001). HeLa cells were plated 1 day before transfection in 5 cm dishes (~4×10⁵ cells/dish). On the day of the transfection the cells were ~50% confluent. For transfection, 10 µl of siRNA duplex (40 µM) was diluted in 350 µl of DMEM in tube 1. In tube 2, 6 µl of OligoFectamine (Invitrogen, Carlsbad, CA) was added to 50 µl of DMEM, and incubated for 10 minutes at room temperature. Tubes 1 and 2 were mixed and incubated for 20 minutes at room temperature. After incubation, the mixture was added to cells grown in 1.6 ml of DMEM. After 3-4 hours, a mixture of FCS, penicillin and streptavidin was added to give the final concentrations indicated above. The cells were incubated for 72 hours in the presence of the siRNA oligos. Then cells from each 5 cm dish were re-plated into two new dishes and incubated for another 72 hours in the absence of siRNA. The cells were lysed and analysed by SDS/PAGE and immunoblotting with anti-Alix antibodies. The blots were quantified using ImageQuant 5.0.

Confocal fluorescence microscopy

HeLa cells grown on coverslips were either permeabilised with 0.05% saponin and fixed with 3% paraformaldehyde or fixed before permeabilisation as indicated. For the staining, various antibodies were used as indicated in the figure legends. Coverslips were examined using a Zeiss LSM 510 META microscope equipped with a Neo-Fluar 100×/1.45 oil immersion objective. Image processing was carried out with Adobe Photoshop version 7.0.

Antibodies

Antibodies against Alix were prepared by immunising a rabbit with

recombinant MBP-Alix fusion protein and affinity-purifying the antiserum on Affi-Gel beads (BioRad) containing immobilised Alix. Affinity-purified rabbit antibodies against recombinant Hrs have been described previously (Raiborg et al., 2001a). A mouse monoclonal antibody against Tsg101 was obtained from GeneTex (San Antonio, TX). A mouse monoclonal antibody against α -tubulin was from Sigma. Human anti-EEA1 antiserum (Mu et al., 1995) was a gift from B. H. Toh (Monash University, Melbourne, Australia). Rabbit antibodies against human LAMP-1 were provided by G. Griffiths (University of Oxford, Oxford, UK). Mouse monoclonal antibodies against LBPA (Kobayashi et al., 1998) were provided by J. Gruenberg (University of Geneva, Geneva, Switzerland). CD63 antibody was from Developmental Studies Hybridoma Bank (University of Iowa, IA). Anti-Rab11 was obtained from Zymed Laboratories (South San Francisco, CA). Sheep antibodies against EGF receptor were from Fitzgerald (Concord, MA). Biotinylated dextran was from Molecular Probes (Oregon, USA). Rhodamine phalloidin was from Molecular Probes (Oregon, USA). Streptavidin-FITC was from Jackson ImmunoResearch Laboratories (West grove, PE). Anti-cortactin (4F11) antibody was from Upstate Biotechnology. Anti-TGN46 was from Serotec. Anti-clathrin heavy chain (X22) was from Affinity BioReagents. Cy2-, Cy3-, Cy5-, FITC- and RRRX-conjugated secondary donkey or goat antibodies were from Jackson ImmunoResearch Laboratories (West Grove, PE).

Transferrin endocytosis and recycling

HeLa cells were transfected with siRNA against Alix or a scrambled RNA duplex of the same nucleotides as control as described above. For the immunofluorescence experiments, the cells were washed in HEPES medium and incubated in HEPES medium for 30 minutes. The cells were then incubated with Alexa594-Transferrin (50 µl/ml; Molecular Probes, Eugene OR) in HEPES medium containing 2 mg/ml of BSA for 5 minutes at 37°C. The cells were washed twice in HEPES medium before chasing for 15 minutes. The cells were then washed with ice-cold phosphate-buffered saline (PBS), fixed with 3% paraformaldehyde and analyzed by confocal fluorescence microscopy. Binding, endocytosis and recycling of Tf were measured using the ORIGIN analyser (IGEN, Rockville, MD), which is based on electrochemiluminescence detection. Human holo-Tf (Sigma, St Louis, MO) was labelled with *N*-hydroxysuccinimide ester-activated tris (bipyridine)-chelated ruthenium(II) (Ru-tag) (IGEN) according to the manufacturer's instructions, and simultaneously labelled with the reducible NHS-SS-Biotin (Pierce). Only Tf that is Ru-tag-labelled and still biotinylated is detected in the cell lysate using streptavidin beads (Dyna, Oslo, Norway). For the binding experiments, the cells were washed twice with HEPES medium and incubated with Ru-tag/SS-biotin labelled transferrin for 1 hour on ice. For the endocytosis experiments, cells were incubated with Ru-tag-labelled-Tf for 2.5, 5 or 7.5 minutes at 37°C. After the incubation times, some of the cells were treated with 0.1 M 2-mercaptoethanesulfonic acid (MESNA) to remove biotin from surface-bound Tf. Ru-tag-Tf recovered from cells treated with MESNA corresponds to the amount of endocytosed Tf, while Ru-tag-Tf from untreated cells corresponds to the total amount of Tf associated with the cells. For the recycling experiments, cells were incubated with Ru-tag/SS-biotin-labelled-Tf for 10 minutes, and then washed and chased at 37°C for 5, 10 and 15 minutes, and surface-bound Ru-tag/SS-biotin-Tf was reduced with MESNA.

Assay of fluid-phase endocytosis

HeLa cells were transfected with siRNA against Alix or a scrambled RNA duplex of the same nucleotides as control as described above for 72 hours in the presence of the siRNA oligos and for another 72 hours in the absence of siRNA in 10% medium. The cells were incubated in the presence of biotinylated dextran (5 mg/ml) for 30 minutes at 37°C and then washed once with medium at 37°C.

The cells were permeabilised before fixation and stained for confocal microscopy using FITC-conjugated streptavidin (Jackson ImmunoResearch).

Assay of EGF receptor degradation

HeLa cells were incubated with medium containing 200 ng/ml EGF and 10 µg/ml cycloheximide for 0 hours and 6 hours before the cells were lysed in lysis buffer. The lysates were analyzed by SDS/PAGE and subsequent immunoblotting using antibodies against the EGF receptor, Alix and tubulin to verify equal loadings.

Electron microscopy

Cells were fixed in a mixture of 4% formaldehyde and 0.1% glutaraldehyde in 0.1 M phosphate buffer (pH 7.4) for 2 hours at room temperature. The cells were then washed in phosphate buffer and scraped off the dish in 1% gelatin/PBS, pelleted and embedded in 10% gelatin/PBS (Peters et al., 1991). Small blocks were cut and infused with 2.3 M sucrose for 1 hour, mounted on silver pins and frozen in liquid nitrogen. Ultrathin cryosections were cut at -110°C on a Leica Ultracut and collected with a 1:1 mixture of 2% methyl cellulose and 2.3 M sucrose. Sections were transferred to formvar/carbon-coated grids and labelled with primary antibodies followed by a bridging secondary antibody and Protein A-gold conjugates essentially as described (Slot et al., 1991). Sections were observed 80 kV in a Philips CM10 electron microscope. Quantification of labelling was performed by counting gold particles on randomly chosen endosomes and total cell profiles. We quantified around 15 cell profiles and endosomes in control and RNAi-treated cells in a total of four or six separate experiments for LBPA and CD63 labelling respectively.

Results

Alix depletion induces perinuclear clustering of endosomes

To study the biological function of Alix *in vivo*, we wanted to reduce the expression of endogenous Alix by using RNA interference (Elbashir et al., 2001; Matsuo et al., 2004). HeLa cells were transfected with siRNA oligonucleotides against Alix or with a scrambled sequence of the same nucleotides. Immunoblot analysis showed that siRNA oligos against Alix caused the strongest depletion of the protein levels after 144 hours (72 hours in the presence of siRNA followed by 72 hours in the absence of RNA, Fig. 1A). The downregulation efficiency was quantified and found to be 90% ($\pm 2\%$; $n=5$) of the total Alix after this treatment. The silencing of Alix seemed to be specific because expression levels of other proteins involved in MVB sorting, such as Hrs and Tsg101, were not affected (Fig. 1B).

In the endocytic pathway, MVBs form from early endosomes and fuse with late endosomes or lysosomes (Gruenberg and Stenmark, 2004; Katzmann et al., 2002). The yeast Alix homolog Bro1 encodes a cytoplasmic protein that associates with endosomal compartments and functions in concert with components of the ESCRT machinery and a deubiquitinating enzyme to regulate MVB formation (Luhtala and Odorizzi, 2004; Odorizzi et al., 2003). We therefore studied the effect of Alix depletion on endocytic compartments in HeLa cells using immunofluorescence microscopy with antibodies against the early-endosomal markers EEA1 and Hrs (Mu et al., 1995; Raiborg et al., 2001), and the late-endosomal/lysosomal markers LBPA and LAMP-1 (Kobayashi et al., 1998; Rabinowitz et al., 1992). In cells treated with

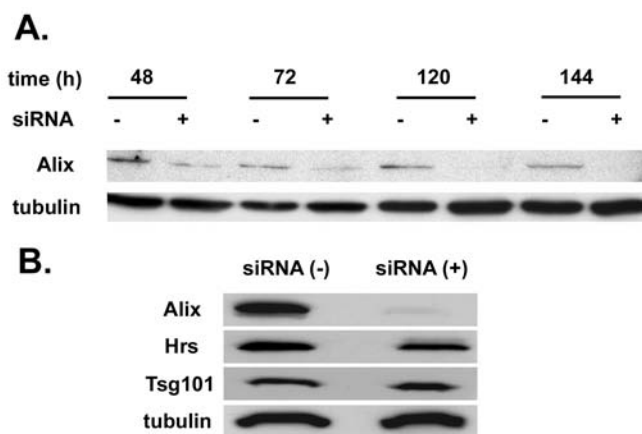


Fig. 1. Downregulation of Alix expression in HeLa cells by siRNA. (A) HeLa cells were treated with control RNA (-) or with siRNA against Alix (+) for the incubation times indicated. The cells were lysed and analysed by SDS/PAGE and immunoblotting with anti-Alix antibodies. Anti- α -tubulin antibodies were used to verify equal loadings. (B) Same experiment as in A, but the incubation time was 72 hours in the presence of siRNA, followed by 72 hours without siRNA. The amounts of Alix, Hrs, Tsg101 and α -tubulin in cell lysates are shown.

control RNA oligonucleotides, early endosomes were dispersed throughout most of the cell (Fig. 2A,B), and LBPA- or LAMP-1-positive structures were found in the perinuclear region, as expected (Fig. 2C,D). However, in cells treated with siRNA against Alix, EEA1-positive endosomes were concentrated in the perinuclear area, with hardly any endosomes in the periphery (Fig. 2E). The other early-endosomal marker, Hrs, also accumulated in the perinuclear area, although some Hrs-positive structures could still be found in the periphery of the cell (Fig. 2F). This siRNA-induced change in early-endosome distribution could be reversed by overexpression of Alix (not shown). The localization of LBPA (Fig. 2G) and LAMP-1 (Fig. 2H) also appeared to be more perinuclear upon Alix depletion, although these results were less conclusive as late endosomes have a perinuclear localization even in control cells. We also noted that the LBPA staining was weaker in Alix-depleted cells (Matsuo et al., 2004) (see later). To verify this effect in another cell line, we studied HepII cells treated with siRNA against Alix. We could observe the same redistribution of early and late (CD63) endosomal markers in the perinuclear region (Fig. 3).

Internalised receptors are delivered to early endosomes, where efficient sorting occurs. Some of the receptors, such as transferrin (Tf) receptors, are rapidly recycled back to the plasma membrane, whereas receptors to be downregulated are transported via the MVB pathway to late endosomes and lysosomes for degradation. To study if the recycling endosomes could also be affected by the depletion of Alix, we monitored the localisation of the GTPase Rab11 (a marker of recycling endosomes) and internalised Tf-Alexa⁵⁹⁴ in Alix-depleted cells. In cells depleted of Alix, internalised Tf-Alexa⁵⁹⁴ accumulated in perinuclear Rab11-positive structures together with EEA1, while the distribution of recycling endosomes was more dispersed in the control cells (Fig. 4). This Tf-Alexa⁵⁹⁴ accumulation was not due to a complete exit

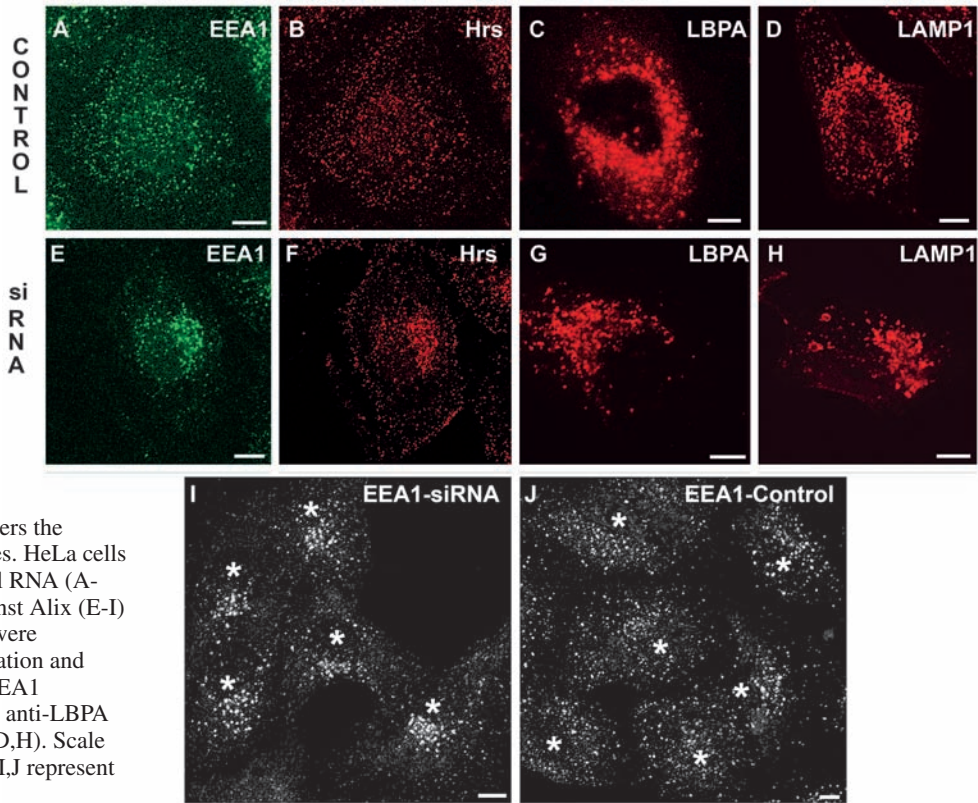


Fig. 2. Alix depletion alters the distribution of endosomes. HeLa cells were treated with control RNA (A-D, J) or with siRNA against Alix (E-I) as in Fig. 1B. The cells were permeabilised before fixation and were stained with anti-EEA1 (A, E, I, J), anti-Hrs (B, F), anti-LBPA (C, G), or anti-LAMP1 (D, H). Scale bars: 5 μ m. Asterisks in I, J represent nuclei.

block, because the labelled transferrin could leave the cells after longer chase times (see later). These results indicate that Alix plays a role in the intracellular positioning of endosomes.

Perinuclear clustering of endosomes induced by Alix depletion does not interfere with transferrin endocytosis and recycling

To investigate whether the striking perinuclear accumulation of

endosomes in Alix-depleted cells alters endocytic membrane trafficking, we used Tf as a marker to follow internalised material through the endocytic/recycling pathways in an electrochemiluminescence-based assay. Tf remains bound to its receptor throughout endocytosis and recycling, which makes it a useful marker for this type of experiment. Relative numbers of Tf-binding sites were determined by incubating cells with Tf at 4°C (at which temperature endocytosis is blocked) for 1 hour. No differences were observed in the

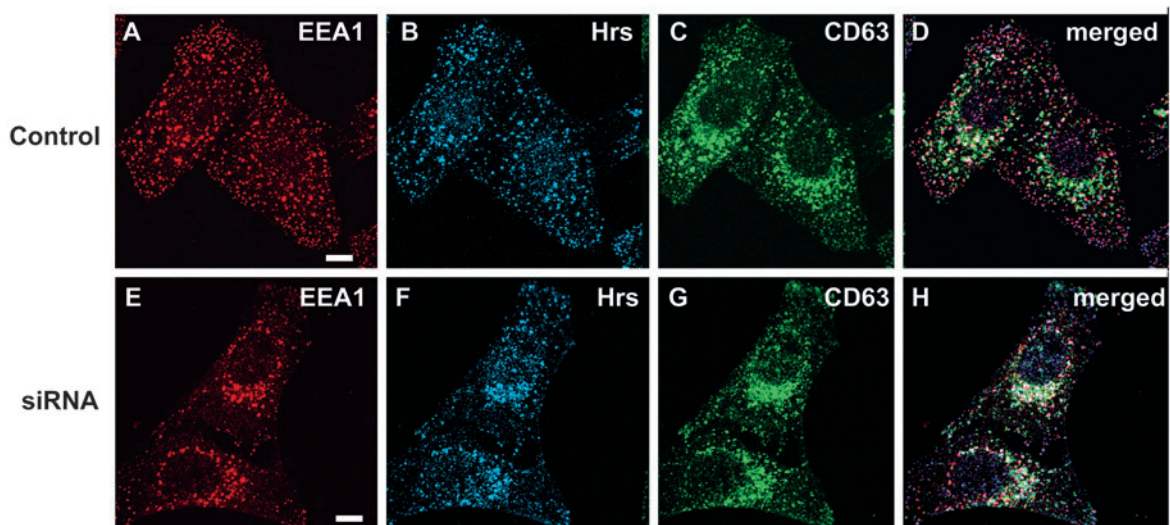


Fig. 3. Alix depletion increases de-colocalisation of early and late endosomal markers in the perinuclear region. HepII cells were treated with control RNA (A-D) or with siRNA against Alix (E-H) as in Fig. 1B. The cells were permeabilised before fixation and were stained with anti-EEA1 (A, E), anti-Hrs (B, F) and anti-CD63 (C, G). Scale bars: 5 μ m.

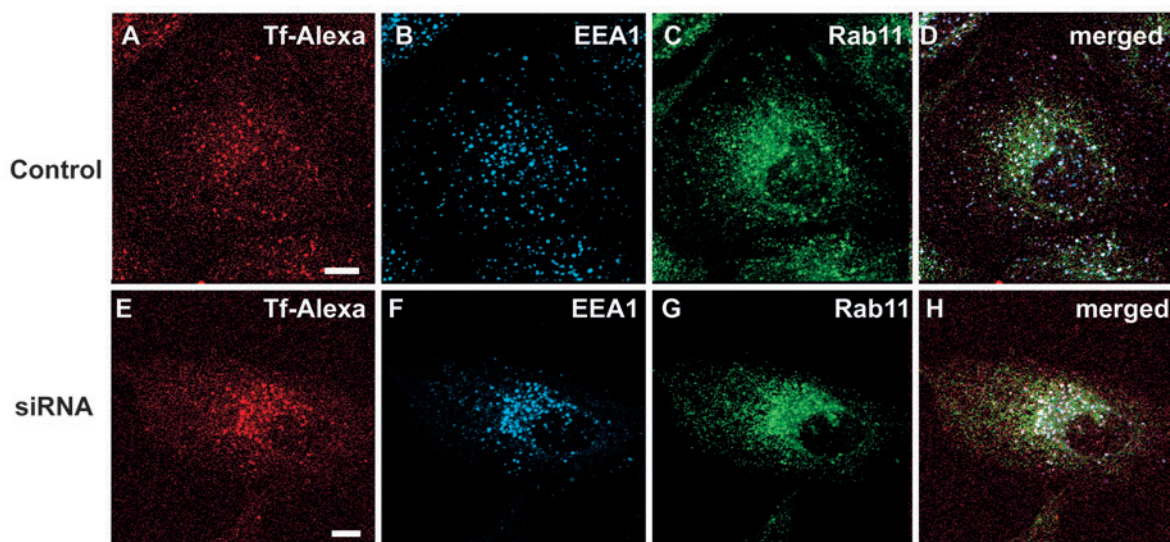


Fig. 4. Alix depletion alters the distribution of transferrin-positive recycling endosomes. HeLa cells were treated with control RNA (A-D) or with siRNA against Alix (E-H) as in Fig. 1B. The cells were incubated with Tf-Alexa⁵⁹⁴ at 37°C for 5 minutes followed by a 15-minute chase to label the recycling endosomes (A,E). The cells were fixed before permeabilisation and were stained with anti-EEA1 (B,F) and anti-Rab11 (C,G). D and H are merged images of B,C and F,G, respectively. White colour indicates colocalisation between Tf-Alexa⁵⁹⁴, EEA1 and Rab11. Scale bars: 5 µm.

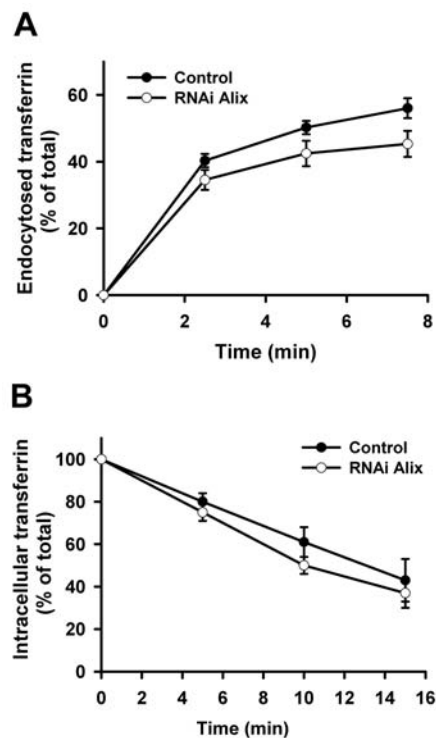
control cells when compared with the cells treated with siRNAs against Alix (data not shown). For the endocytosis or uptake experiments, cells were incubated with Tf for different time points and the intracellular transferrin was measured with respect to total cell-associated transferrin. Alix-depleted cells showed a minor decrease in Tf internalisation in comparison with control cells (Fig. 5A). In the recycling experiments, the cells were incubated for 10 minutes with Tf and chased for different time points. Compared with the Tf recycling in control cells, Alix depletion caused no significant changes (Fig. 5B). These results indicate that the proper distribution of early and recycling endosomes is not rate-limiting for recycling of transferrin.

Depletion of Alix does not affect EGF receptor trafficking to the late endocytic pathway

Alix has been reported to interact with Tsg101 and CHMP4, components of the ESCRT-I and -III complexes of the MVB sorting pathway (Kato et al., 2003; von Schwedler et al., 2003). It is known that decreased levels of ESCRT-I proteins result in accumulation of endocytosed EGF or affect EGF

receptor downregulation (Babst et al., 2000; Bache et al., 2004; Bishop et al., 2002). However, Bro1, the yeast counterpart of Alix, is not essential for ubiquitination or for endocytosis of Gap1, an amino acid permease used as a model cargo to study the trafficking of membrane proteins in yeast (Nikko et al., 2003). Nevertheless, Bro1, has been implicated in MVB sorting, together with the ESCRTs (Katzmann et al., 2002). We therefore asked whether Alix has a function in receptor downregulation, using EGF-induced degradation of EGF

Fig. 5. Effect of Alix depletion on transferrin endocytosis and recycling. HeLa cells were treated with control RNA or with siRNA against Alix as in Fig. 1B. For the endocytosis experiments (A), cells were incubated with Ru-tag-Tf for different times at 37°C as described in the Materials and Methods, and the surface-bound Ru-tag-Tf was reduced with MESNA. The amount of cell-associated Tf was measured using an ORIGEN analyser, and endocytosed Tf is presented as a percentage of total cell-associated Tf. Error bars represent the s.e.m. of three independent experiments performed in duplicate. (B) Cells were incubated with Ru-tag-Tf for 10 minutes and then washed and chased at 37°C for 5, 10 or 15 minutes before MESNA treatment. Error bars represent the s.e.m. of three independent experiments performed in duplicate.



receptor as a model system. In our experiments, control HeLa cells or Alix-depleted cells were stimulated with EGF for 30 minutes, and either lysed immediately or following a 6 hour chase. The amounts of EGF receptors were measured by western blotting. As a positive control, we used siRNA against the ESCRT-I subunit HCRP1, which has been shown to be essential for ligand-induced EGF receptor degradation (Bache et al., 2004). Our experiments showed that, whereas HCRP1 depletion inhibited EGF receptor downregulation, this was not the case with Alix depletion (Fig. 6). These results agree with a recent report (Schmidt et al., 2004b) and suggest that Alix is not essential for efficient sorting of the EGF receptor into the MVB pathway.

Alix depletion affects the accumulation of LBPA but not CD63 in multivesicular endosomes

In order to study whether Alix depletion influences the subcellular distribution of endosomal markers, we performed immunocytochemistry on thawed cryosections. A previous study has implicated a role for Alix as a regulator of LBPA-mediated MVB biogenesis. This study revealed a reduction of total cellular and endosomal LBPA content upon RNAi against Alix (Matsuo et al., 2004). We decided to compare the amounts of LBPA with those of an integral membrane protein in multivesicular endosomes, in order to understand whether Alix depletion causes a general sorting defect or whether LBPA sorting or metabolism specifically is disturbed. For this purpose, we chose CD63 as a marker, because of its high enrichment in multivesicular endosomes (Escola et al., 1998).

Immunolabelling of control and RNAi-treated cells showed that both markers, LBPA and CD63, localised to multivesicular structures presumably corresponding to late endosomes (Fig. 7A-D). We were unable to detect any morphological changes of endosomes caused by Alix depletion, although we cannot exclude the possibility that the number of intraluminal vesicles was affected. The total cellular and endosomal labelling densities of LBPA seemed to be reduced in Alix-depleted cells. We did not, however, observe any obvious changes in the CD63 distribution. To verify these observations, we performed a quantification of both labelling patterns. This analysis confirmed our initial observations (Fig. 7E,F). The CD63

labelling in Alix-depleted cells was not significantly reduced when compared with control cells, whereas the LBPA labelling was reduced by 60% in total cell content and by 40% for endosomal content, reductions that were statistically significant. These results agree with a previous report that Alix is required for normal LBPA levels in late endosomes (Matsuo et al., 2004) and with our finding (Fig. 6) that Alix is not essential for sorting of membrane proteins from early to late endosomes. Even though we did not quantify the number of late endosomes, it is interesting to note that the siRNA-mediated reduction in cellular LBPA content was greater than the reduction in endosomal LBPA content. This is in agreement with a previous finding that Alix depletion causes a reduction in the number of LBPA-positive late endosomes (Matsuo et al., 2004).

Downregulation of Alix results in unusual cortical actin structures that colocalise with cortactin and clathrin heavy chain

As Alix has been reported to associate with proteins of the cytoskeleton, including actin and tubulins (Schmidt et al., 2003), we asked whether Alix is important for the organisation of the actin cytoskeleton. To address this, HeLa cells were treated with siRNA against Alix and stained with rhodamine-phalloidin to visualise actin by fluorescence microscopy. Interestingly, an abnormal actin organisation was observed in the Alix-depleted cells (Fig. 8E, see also Fig. 9C and Fig. 10B) in contrast to the normal F-actin staining in the control cells (Fig. 8B, see also Fig. 9A and Fig. 10A). These unusual structures had a variety of forms, but most of them looked like rings, small crescents or aggregates of F-actin.

Different actin-associated proteins can be connected to diverse actin-based structures that determine their properties and regulation. We therefore decided to investigate possible proteins that can associate with the F-actin structures to obtain some information of their origin. Cortactin is an actin-binding protein that couples membrane dynamics to the cortical actin cytoskeleton (Weed and Parsons, 2001), and in order to investigate whether the aberrant actin structures contained this protein, we stained Alix-depleted cells with an antibody that detects endogenous cortactin. Confocal microscopy showed that the aberrant actin structures labelled strongly for cortactin (Fig. 8E,F). This suggests that Alix is required for a proper organisation of the cortical actin cytoskeleton.

Cortactin has recently been implicated in membrane dynamics and actin cytoskeletal functions. It directly activates the Arp2/3 complex, which nucleates assembly of new actin filaments at endocytic sites. Moreover, cortactin inhibits debranching of the resulting filament networks in vitro and is a component of clathrin-coated pits (Engqvist-Goldstein and Drubin, 2003). Clathrin is one of the coat proteins that together with an inner shell of 'assembly proteins' form the coat of vesicles involved in endocytosis as well as traffic from endosomes and the *trans*-Golgi network (TGN) (Brodsky et al., 2001; Kirchhausen, 2000). Because of the reported localisation of cortactin to clathrin-coated pits, we investigated whether the cortactin-

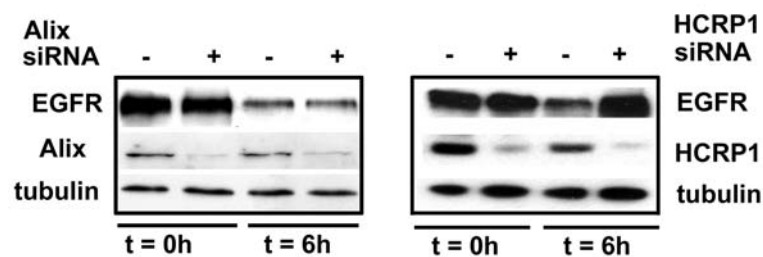


Fig. 6. Depletion of Alix does not inhibit EGF receptor downregulation. HeLa cells treated with control RNA (-) or with siRNA (+) against Alix (see Fig. 1B) or with siRNA (+) against HCRP1. The cells were stimulated for 30 minutes with EGF 200 ng/ml (time 0), and then washed and chased for 6 hours in the presence of 10 μ g/ml cycloheximide before the cells were lysed in lysis buffer. The lysates were analyzed by SDS/PAGE and sequential blotting with antibodies against EGF receptor, Alix and HCRP1. The same membrane was then reblotted with anti-tubulin to verify equal loadings. The experiment was repeated three times with the same result.

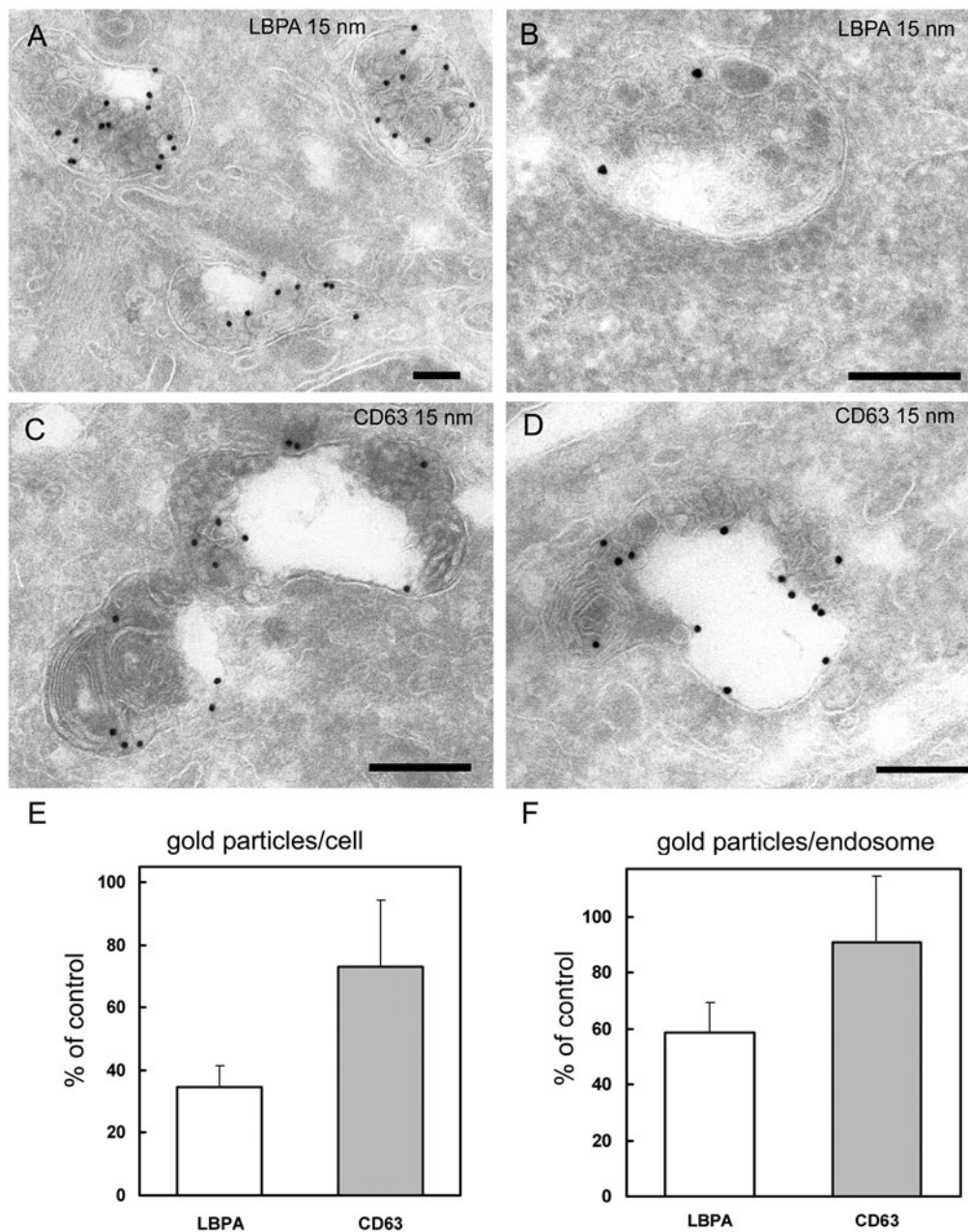


Fig. 7. Alix depletion affects LBPA but not CD63 levels in multivesicular endosomes. Subcellular localisation of LBPA and CD63 in control (A,C) and Alix-siRNA-treated (B,D) cells. Cells were labelled with monoclonal antibodies against LBPA and CD63 followed by a rabbit anti-mouse antibody and 15 nm protein A gold. In control cells, LBPA was found in typical MVBs and multilamellar late endosomes. Less staining was observed in Alix-siRNA-treated cells. CD63 labelling was also found in MVBs and late endosomes. Quantitation of the labelling intensity (E,F) indicated that total cell and endosomal LBPA content was significantly reduced, whereas CD63 levels were close to control values. Scale bars: 200 nm.

containing aberrant actin structures in Alix-depleted cells contained clathrin. Confocal microscopy indicated that this was the case (Fig. 9C,D). This suggests that Alix plays a role in coordinating the interactions between the cortical actin cytoskeleton and the endocytic machinery.

Even though we had the impression that the unusual actin-positive structures induced by Alix depletion accumulated close to the plasma membrane, we could not exclude the possibility that they represented endosomes. To address this, we first studied whether these structures, labelled with phalloidin, colocalised with EEA1, Hrs or LAMP1, but no colocalisation was found (data not shown). We next studied if these structures were accessible to a fluid-phase marker, biotinylated dextran. As shown in Fig. 10, there was no colocalisation between the siRNA-induced actin structures and internalised biotin-dextran. These results suggest that

the unusual phalloidin-positive structures represent submembraneous actin patches.

A similar actin phenotype has been reported in cells depleted for the actin- and clathrin-binding protein Hip1R (see Discussion). Depletion of Hip1R not only caused the formation of unusual actin structures but also resulted in disruption of the characteristic perinuclear TGN organisation (Carreno et al., 2004; Engqvist-Goldstein et al., 2004). To study whether Alix downregulation could have any effect in the TGN, siRNA-treated cells were stained with the TGN marker TGN46. No difference in the localisation of TGN46 was observed in the Alix-depleted cells with respect to the control cells (data not shown). This suggests that Alix, unlike Hip1R, does not control budding of clathrin-coated vesicles from the TGN. In conclusion, the fact that depletion of Alix resulted in abnormal actin structures containing both an actin polymerisation factor

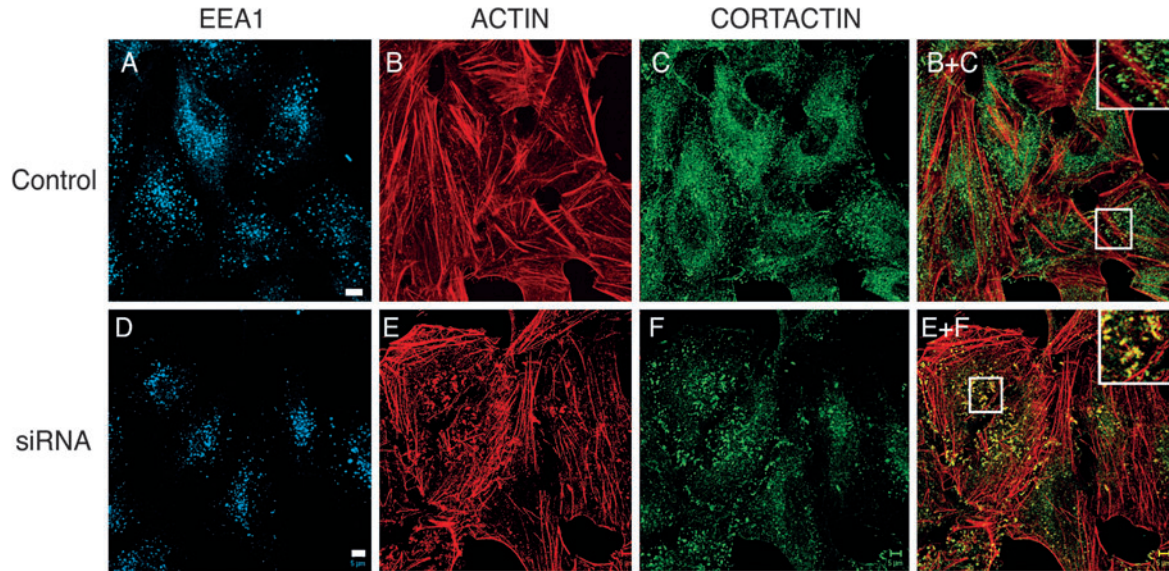


Fig. 8. Accumulation of abnormal cortical actin structures in response to lowered Alix levels. HeLa cells treated with control RNA (A-C) or with siRNA (D-F) against Alix (see Fig. 1B) were stained with rhodamine-phalloidin (B-E), anti-cortactin (C-F) and anti-EEA1 (A-D). Yellow shows colocalisation between actin and cortactin in abnormal actin structures. Scale bars: 5 μ m.

(cortactin) and an endocytic component (clathrin) suggests that Alix plays a role in connecting the endocytic machinery to actin.

Discussion

In this report, we have used the siRNA approach to elucidate the role of Alix in the MVB pathway. The Alix-depleted cells showed a strong perinuclear redistribution of early endosomes and recycling endosomes, whereas late endosomes appeared to be less affected. As the latter endosomes have a perinuclear distribution even in untreated cells, eventual effects on these endosomes induced by Alix depletion may be more difficult to

detect. We were surprised to find that the redistribution of endosomes caused by Alix depletion only had a minimal effect on Tf uptake and did not inhibit Tf recycling or EGF degradation. However, the finding that a striking alteration in the distribution of endosomes has minor effects on endosomal trafficking has some precedents. Similar effects have been observed upon depletion of the actin-binding protein annexin II (Zobiack et al., 2003) or overexpression of the clathrin hub domain (Bennett et al., 2001b). In future experiments, it will be interesting to establish whether Alix may function in concert with annexin II and clathrin to regulate the spatial distribution of endosomes.

Like depletion of Alix, overexpression of the clathrin hub

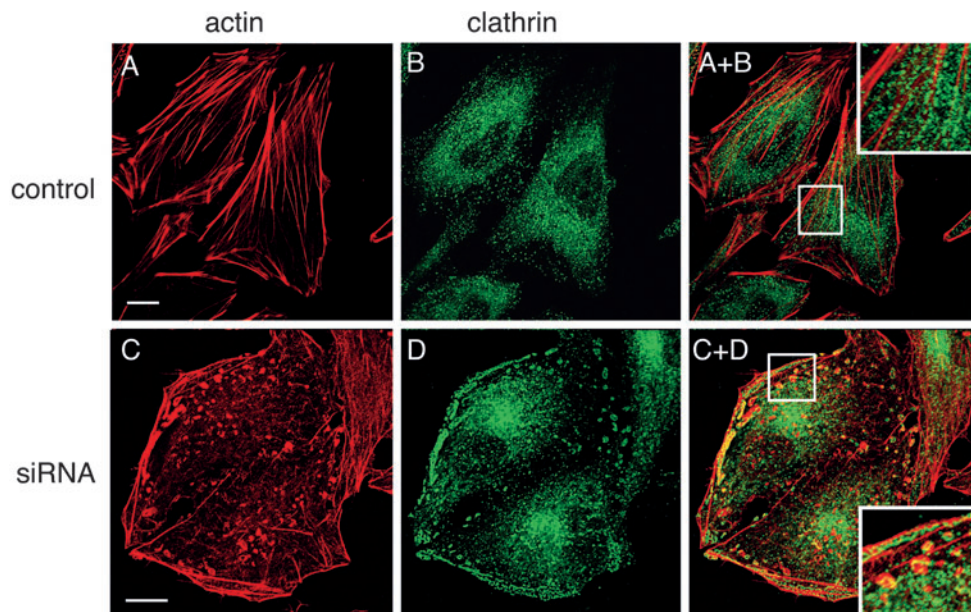


Fig. 9. The F-actin structures that accumulate in Alix-depleted cells colocalise with clathrin. HeLa cells treated with control RNA (A,B) or with siRNA (C,D) against Alix (see Fig. 1B) were stained with rhodamine-phalloidin (A-C) and anti-clathrin (B-D). Yellow indicates colocalisation between actin and clathrin. Scale bars: 5 μ m.

domain in HeLa cells causes a perinuclear localisation of early endosomes (Bennett et al., 2001b). The hub domain comprises the C-terminal third of clathrin heavy chain and has been shown to act as a dominant-negative clathrin inhibitor by competing for light-chain binding (Liu et al., 1998; Liu et al., 1995). Clathrin hub expression leads to dissociation of the actin-binding protein Hip1R from coated pits, and disrupts the alignment with the actin cytoskeleton. This suggests a role for the clathrin-Hip1R interaction in mediating the spatial relationship between endosomes and the cortical actin cytoskeleton (Bennett et al., 2001a). Even though overexpression of the clathrin hub domain inhibits Tf endocytosis, it does not significantly affect endocytic recycling (Bennett et al., 2001b). This shows that the positioning of endosomes is not crucial for this cellular function.

A similar example where Tf-receptor-containing recycling endosomes are clustered in the perinuclear area has been shown in HeLa cells depleted of annexin II or the annexin II-S100A10 complex (Zobiack et al., 2003). Annexin II belongs to a group of cytosolic Ca^{2+} -binding proteins that cycle between the cytosol and specific target membranes. This protein is recruited to the plasma membrane and to endosomal membranes, and interacts directly with polymerised actin *in vitro* (Gerke and Moss, 2002; Hayes et al., 2004). It is not known whether Alix can bind clathrin or annexin II, but it is interesting to note that the Alix-interacting protein ALG-2 has been found to interact with other annexins (VII and XI) (Sato et al., 2002), and Alix interacts with proteins involved in clathrin-coated pit formation, such as endophilin and CIN85 (Chatellard-Causse et al., 2002; Schmidt et al., 2003). It therefore seems that this phenotype is produced by a lack of proteins associated with actin and the endocytic machinery. As with Alix depletion and clathrin hub overexpression, the endosome redistribution caused by annexin II depletion was not associated with any effects on endocytic recycling (Bennett et al., 2001b; Zobiack et al., 2003). In addition, the rate of endocytosis was unaffected, and no difference in lysosomal trafficking of endocytosed LDL could be detected in annexin II-depleted cells (Zobiack et al., 2003). Thus, the functional consequences of annexin II depletion appear to be very similar

to those of Alix depletion. These examples demonstrate that the intracellular positioning of endosomes is not limiting for endocytic recycling and that Alix does not play an essential role in the sorting and recycling pathway in HeLa cells. Possibly, the exact positioning of early and recycling endosomes might be of minor importance in non-polarised cells grown as monolayer cultures, because their distance to the plasma membrane would be short anyway. The situation could be different in cells that have a more polarised distribution of endosomes, such as neurons.

Previous work has connected Alix with the endocytic machinery through its interactions with Tsg101 and CHMP4 from ESCRT-I and ESCRT-III (Katoh et al., 2004; Katoh et al., 2003; von Schwedler et al., 2003), and with the late-endosomal lipid LBPA (Matsuo et al., 2004). Alix also binds the Gag proteins of HIV-1 and EIAV (von Schwedler et al., 2003). The involvement of Alix in viral budding is virus dependent as siRNA against Alix dramatically inhibits EIAV budding, whereas infectious HIV-1 production is less affected (Martin-Serrano et al., 2003). Concerning the effect of Alix in late endocytic compartments, we show in this paper that downregulation of Alix leads to a decrease of LBPA in late endosomes, in agreement with a previous report (Matsuo et al., 2004). However, Alix depletion did not reduce the CD63 content of MVBs and late endosomes, and it did not interfere with ligand-induced EGF receptor downregulation. It has been proposed that Alix regulates the dynamics of intraluminal vesicles within MVBs and late endosomes (Matsuo et al., 2004). Consistent with this, Alix depletion inhibits release of the lethal factor of anthrax toxin from MVBs. This release process is thought to involve sorting of the toxin into intraluminal vesicles, followed by release into cytosol upon fusion of the vesicles with the limiting membrane of the MVB (Abrami et al., 2004). If Alix indeed controls the motility of intraluminal vesicles in MVBs, this could explain why Alix depletion fails to inhibit EGF receptor degradation, as the receptor would still be exposed to lysosomal enzymes as long as it is located within the membrane of the intraluminal vesicles of the MVB. During the submission of this manuscript, it was also proposed that Alix inhibits EGF receptor internalisation and antagonises the promotion of EGF receptor downregulation by the Cbl-SETA/CIN85 complex, but does not profoundly affect EGF receptor degradation (Schmidt et al., 2005; Schmidt et al., 2004), which fits with our observations concerning EGF receptor degradation. Further studies are needed to understand how Alix might control the motility of intraluminal endosomal vesicles, and whether this function would be related to its regulation of the actin cytoskeleton.

When trying to elucidate the function of Alix, it is informative to consider its yeast homologue, Bro1. In yeast, the sorting of proteins into the vacuolar lumen via the MVB pathway requires the class E Vps proteins, most of which are organised in three ESCRTs. In class E *vps* mutants, the proteins that enter the endocytic pathway accumulate in an aberrant late endosome called the class E compartment and/or are mis-sorted to the vacuole limiting membrane (Babst et al., 2002a; Babst et al., 2002b; Katzmann et al., 2001). In *bro1Δ* yeast, the class E compartment is less prominent than in other *vpsΔ* cells (Nikko et al., 2003). The membrane permease Gap1 accumulates in the class E compartment and is not targeted to

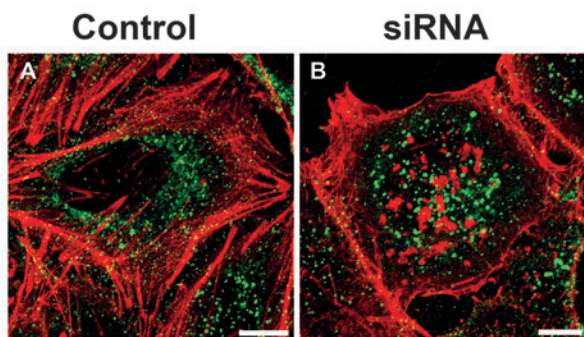


Fig. 10. The F-actin structures that accumulate in Alix-depleted cells are not accessible to fluid phase markers. HeLa cells were treated with control RNA (A) or with siRNA (B) against Alix (see Fig. 1B). The cells were left to internalise biotinylated dextran (5 mg/ml) for 30 minutes at 37°C, and then washed once with medium at 37°C. The cells were permeabilised before fixation on ice and stained for confocal microscopy using FITC-streptavidin (green) and rhodamine-phalloidin (red). Scale bars: 5 μm.

the vacuolar lumen in *vpsΔ* cells. However, Gap1 is internalised and then recycled back to the cell surface in *bro1Δ* cells, a process that might depend on normal endosome-to-vacuole fusion. The 'mild' *vps* class E phenotype of *bro1Δ* yeast is consistent with the failure of Alix depletion to inhibit EGF receptor degradation and CD63 trafficking in mammalian cells.

It has been reported previously that Alix associates with microtubules and actin filaments, although it is not clear whether this is due to a direct interaction (Schmidt et al., 2003). Our results support the view that Alix is involved in actin regulation, as unusual actin-positive structures that colocalised with cortactin and clathrin were formed in Alix-depleted cells. Because these structures were not accessible to a fluid-phase marker, they are unlikely to represent endosomes and they probably correspond to cortical actin patches at the plasma membrane. Of note, Alix interacts with the tyrosine kinases FAK and Pyk2 in adherent cells and negatively regulates cell adhesion and focal adhesion kinase activity (Schmidt et al., 2003), and reduction of Alix levels can increase cell adhesion (Schmidt et al., 2004a). Perhaps the increased adhesion upon Alix depletion might be related to the increased patches of cortical actin. A similar phenotype has been previously reported in HeLa cells with decreased levels of Hip1R. Abnormal F-actin structures were observed in the Hip1R-depleted cells, and cortactin, clathrin and other endocytic components were associated with these (Engqvist-Goldstein et al., 2004). Hip1R is a component of clathrin-coated pits and clathrin-coated vesicles, and its ability to bind simultaneously both F-actin and clathrin has raised the possibility that Hip1R links actin cytoskeletal functions and receptor-mediated endocytosis (Engqvist-Goldstein and Drubin, 2003). Hip1R and the related protein Hip1 have been implicated in endocytosis or trafficking of clathrin-coated vesicles. Depletion of Hip1R in HeLa cells has a weak inhibitory effect on transferrin uptake (Engqvist-Goldstein et al., 2004). Likewise, in Alix-depleted cells, in which the actin cytoskeleton appeared to be affected in a similar way to that in Hip1R-depleted cells, we observed a minor inhibition of Tf endocytosis. However, whereas Hip1R depletion disrupts the organisation of the TGN (Carreno et al., 2004), we did not observe any such effect in Alix-depleted cells. Therefore, Hip1R and Alix are likely to play distinct roles in coordinating the actin cytoskeleton with membrane dynamics.

Recent studies have suggested that Alix is able to bind directly to the Tf receptor and indirectly to the EGF receptor, and that it controls exosomal shedding of the Tf receptor and endocytosis of the EGF receptor, respectively (Geminard et al., 2004; Schmidt et al., 2004b). Even though the underlying mechanisms have not been clarified, it is tempting to speculate that the ability of Alix to control cortical actin may contribute to its involvement in exosomal shedding and endocytosis. In line with this, Alix has been found together with actin in purified exosomes (Wubbolts et al., 2003), and there is a well-documented involvement of actin in endocytosis (Hayes et al., 2004).

In conclusion, depletion of Alix yields effects that are partially reminiscent to depletion of annexin II or Hip1R or overexpression of the clathrin hub domain. Moreover, Alix depletion induces the formation of aberrant actin structures that contain cortactin and clathrin. Annexin II, Hip1R and cortactin

are all actin-binding proteins, and Alix is known to interact with endocytic regulators such as CIN85 and endophilins. Taken together, these data implicate Alix in the interface between the cortical actin cytoskeleton and the endocytic machinery, although its exact function here remains unknown. It will be interesting to elucidate how Alix connects with actin and the actin cytoskeleton. One possible clue comes from the fact that the proline-rich C terminus of Alix contains potential binding sites for SH3- and WW-domains, which are frequently found in regulators of actin function and endocytic trafficking. The identification of such Alix-interacting proteins would serve to shed light on its function.

We thank Jean Gruenberg for kindly providing antibodies against LBPA. This work was supported by the Research Council of Norway, the Norwegian Cancer Society, the Novo Nordisk Foundation and a Marie Curie Research Training Grant (HPRN-CT-2000-00081) from the European Union. A.B. is a career fellow of the FUGE program of the Research Council of Norway.

References

- Abrami, L., Lindsay, M., Parton, R. G., Leppla, S. H. and van Der Goot, F. G. (2004). Membrane insertion of anthrax protective antigen and cytoplasmic delivery of lethal factor occur at different stages of the endocytic pathway. *J. Cell Biol.* **166**, 645-651.
- Amara, A. and Littman, D. R. (2003). After Hrs with HIV. *J. Cell Biol.* **162**, 371-375.
- Babst, M., Odorizzi, G., Estepa, E. J. and Emr, S. D. (2000). Mammalian tumor susceptibility gene 101 (TSG101) and the yeast homologue, Vps23p, both function in late endosomal trafficking. *Traffic* **1**, 248-258.
- Babst, M., Katzmann, D. J., Estepa-Sabal, E. J., Meerloo, T. and Emr, S. D. (2002a). Escrt-III: an endosome-associated heterooligomeric protein complex required for mvb sorting. *Dev. Cell* **3**, 271-282.
- Babst, M., Katzmann, D. J., Snyder, W. B., Wendland, B. and Emr, S. D. (2002b). Endosome-associated complex, ESCRT-II, recruits transport machinery for protein sorting at the multivesicular body. *Dev. Cell* **3**, 283-289.
- Bache, K. G., Brech, A., Mehlum, A. and Stenmark, H. (2003). Hrs regulates multivesicular body formation via ESCRT recruitment to endosomes. *J. Cell Biol.* **162**, 435-442.
- Bache, K. G., Slagsvold, T., Cabezas, A., Rosendal, K. R., Raiborg, C. and Stenmark, H. (2004). The Growth-Regulatory Protein HCRP1/hVps37A is a Subunit of Mammalian ESCRT-I and Mediates Receptor Downregulation. *Mol. Cell Biol.* **15**, 4337-4346.
- Bennett, E. M., Chen, C. Y., Engqvist-Goldstein, A. E., Drubin, D. G. and Brodsky, F. M. (2001a). Clathrin hub expression dissociates the actin-binding protein Hip1R from coated pits and disrupts their alignment with the actin cytoskeleton. *Traffic* **2**, 851-858.
- Bennett, E. M., Lin, S. X., Towler, M. C., Maxfield, F. R. and Brodsky, F. M. (2001b). Clathrin hub expression affects early endosome distribution with minimal impact on receptor sorting and recycling. *Mol. Biol. Cell* **12**, 2790-2799.
- Bishop, N., Horman, A. and Woodman, P. (2002). Mammalian class E vps proteins recognize ubiquitin and act in the removal of endosomal protein-ubiquitin conjugates. *J. Cell Biol.* **157**, 91-101.
- Borinstein, S. C., Hyatt, M. A., Sykes, V. W., Straub, R. E., Lipkowitz, S., Boulter, J. and Bogler, O. (2000). SETA is a multifunctional adapter protein with three SH3 domains that binds Grb2, Cbl, and the novel SB1 proteins. *Cell Signal.* **12**, 769-779.
- Brodsky, F. M., Chen, C. Y., Kneuhl, C., Towler, M. C. and Wakeham, D. E. (2001). Biological basket weaving: formation and function of clathrin-coated vesicles. *Annu. Rev. Cell Dev. Biol.* **17**, 517-568.
- Carreno, S., Engqvist-Goldstein, A. E., Zhang, C. X., McDonald, K. L. and Drubin, D. G. (2004). Actin dynamics coupled to clathrin-coated vesicle formation at the trans-Golgi network. *J. Cell Biol.* **165**, 781-788.
- Chatellard-Cause, C., Blot, B., Cristina, N., Torch, S., Missotten, M. and Sadoul, R. (2002). Alix (ALG-2-interacting protein X), a protein involved in apoptosis, binds to endophilins and induces cytoplasmic vacuolization. *J. Biol. Chem.* **277**, 29108-29115.
- Chen, B., Borinstein, S. C., Gillis, J., Sykes, V. W. and Bogler, O. (2000).

- The glioma-associated protein SETA interacts with AIP1/Alix and ALG-2 and modulates apoptosis in astrocytes. *J. Biol. Chem.* **275**, 19275-19281.
- Dikic, I.** (2004). ALIX-ing phospholipids with endosome biogenesis. *BioEssays* **26**, 604-607.
- Elbashir, S. M., Harborth, J., Lendeckel, W., Yalcin, A., Weber, K. and Tuschl, T.** (2001). Duplexes of 21-nucleotide RNAs mediate RNA interference in cultured mammalian cells. *Nature* **411**, 494-498.
- Engqvist-Goldstein, A. E. and Drubin, D. G.** (2003). Actin assembly and endocytosis: from yeast to mammals. *Annu. Rev. Cell Dev. Biol.* **19**, 287-332.
- Engqvist-Goldstein, A. E., Zhang, C. X., Carreno, S., Barroso, C., Heuser, J. E. and Drubin, D. G.** (2004). RNAi-mediated Hip1R silencing results in stable association between the endocytic machinery and the actin assembly machinery. *Mol. Biol. Cell* **15**, 1666-1679.
- Escola, J. M., Kleijmeer, M. J., Stoorvogel, W., Griffith, J. M., Yoshie, O. and Geuze, H. J.** (1998). Selective enrichment of tetraspan proteins on the internal vesicles of multivesicular endosomes and on exosomes secreted by human B-lymphocytes. *J. Biol. Chem.* **273**, 20121-20127.
- Geminard, C., de Gassart, A., Blanc, L. and Vidal, M.** (2004). Degradation of AP2 during reticulocyte maturation enhances binding of hsc70 and Alix to a common site on TFR for sorting into exosomes. *Traffic* **5**, 181-193.
- Gerke, V. and Moss, S. E.** (2002). Annexins: from structure to function. *Physiol. Rev.* **82**, 331-371.
- Gruenberg, J.** (2001). The endocytic pathway: a mosaic of domains. *Nat. Rev. Mol. Cell Biol.* **2**, 721-730.
- Gruenberg, J. and Stenmark, H.** (2004). The biogenesis of multivesicular endosomes. *Nat. Rev. Mol. Cell Biol.* **5**, 317-323.
- Haglund, K., di Fiore, P. P. and Dikic, I.** (2003). Distinct monoubiquitin signals in receptor endocytosis. *Trends Biochem. Sci.* **28**, 598-603.
- Hayes, M. J., Rescher, U., Gerke, V. and Moss, S. E.** (2004). Annexin-actin interactions. *Traffic* **5**, 571-576.
- Katoh, K., Shibata, H., Suzuki, H., Nara, A., Ishidoh, K., Kominami, E., Yoshimori, T. and Maki, M.** (2003). The ALG-2-interacting protein Alix associates with CHMP4b, a human homologue of yeast Snf7 that is involved in multivesicular body sorting. *J. Biol. Chem.* **278**, 39104-39113.
- Katoh, K., Shibata, H., Hatta, K. and Maki, M.** (2004). CHMP4b is a major binding partner of the ALG-2-interacting protein Alix among the three CHMP4 isoforms. *Arch. Biochem. Biophys.* **421**, 159-165.
- Katzmann, D. J., Babst, M. and Emr, S. D.** (2001). Ubiquitin-dependent sorting into the multivesicular body pathway requires the function of a conserved endosomal protein sorting complex, ESCRT-I. *Cell* **106**, 145-155.
- Katzmann, D. J., Odorizzi, G. and Emr, S. D.** (2002). Receptor downregulation and multivesicular-body sorting. *Nat. Rev. Mol. Cell Biol.* **3**, 893-905.
- Katzmann, D. J., Stefan, C. J., Babst, M. and Emr, S. D.** (2003). Vps27 recruits ESCRT machinery to endosomes during MVB sorting. *J. Cell Biol.* **162**, 413-423.
- Kirchhausen, T.** (2000). Clathrin. *Annu. Rev. Biochem.* **69**, 699-727.
- Kobayashi, T., Stang, E., Fang, K. S., de Moerloose, P., Parton, R. G. and Gruenberg, J.** (1998). A lipid associated with the antiphospholipid syndrome regulates endosome structure and function. *Nature* **392**, 193-197.
- Liu, S. H., Wong, M. L., Craik, C. S. and Brodsky, F. M.** (1995). Regulation of clathrin assembly and trimerization defined using recombinant triskelion hubs. *Cell* **83**, 257-267.
- Liu, S. H., Marks, M. S. and Brodsky, F. M.** (1998). A dominant-negative clathrin mutant differentially affects trafficking of molecules with distinct sorting motifs in the class II major histocompatibility complex (MHC) pathway. *J. Cell Biol.* **140**, 1023-1037.
- Luhtala, N. and Odorizzi, G.** (2004). Bro1 coordinates deubiquitination in the multivesicular body pathway by recruiting Doa4 to endosomes. *J. Cell Biol.* **166**, 717-729.
- Martin-Serrano, J., Yarovoy, A., Perez-Caballero, D. and Bieniasz, P. D.** (2003). Divergent retroviral late-budding domains recruit vacuolar protein sorting factors by using alternative adaptor proteins. *Proc. Natl. Acad. Sci. USA* **100**, 12414-12419.
- Matsuo, H., Chevallier, J., Mayran, N., le Blanc, I., Ferguson, C., Faure, J., Blanc, N. S., Matile, S., Dubochet, J., Sadoul, R. et al.** (2004). Role of LBPA and Alix in multivesicular liposome formation and endosome organization. *Science* **303**, 531-534.
- Missotten, M., Nichols, A., Rieger, K. and Sadoul, R.** (1999). Alix, a novel mouse protein undergoing calcium-dependent interaction with the apoptosis-linked-gene 2 (ALG-2) protein. *Cell Death Differ.* **6**, 124-129.
- Mu, F. T., Callaghan, J. M., Steele-Mortimer, O., Stenmark, H., Parton, R. G., Campbell, P. L., McCluskey, J., Yeo, J. P., Tock, E. P. and Toh, B. H.** (1995). EEA1, an early endosome-associated protein. EEA1 is a conserved alpha-helical peripheral membrane protein flanked by cysteine "fingers" and contains a calmodulin-binding IQ motif. *J. Biol. Chem.* **270**, 13503-13511.
- Nikko, E., Marini, A. M. and Andre, B.** (2003). Permease recycling and ubiquitination status reveal a particular role for Bro1 in the multivesicular body pathway. *J. Biol. Chem.* **278**, 50732-50743.
- Odorizzi, G., Katzmann, D. J., Babst, M., Audhya, A. and Emr, S. D.** (2003). Bro1 is an endosome-associated protein that functions in the MVB pathway in *Saccharomyces cerevisiae*. *J. Cell Sci.* **116**, 1893-1903.
- Peters, P. J., Neefjes, J. J., Oorschot, V., Ploegh, H. L. and Geuze, H. J.** (1991). Segregation of MHC class II molecules from MHC class I molecules in the Golgi complex for transport to lysosomal compartments. *Nature* **349**, 669-676.
- Rabinowitz, S., Horstmann, H., Gordon, S. and Griffiths, G.** (1992). Immunocytochemical characterization of the endocytic and phagolysosomal compartments in peritoneal macrophages. *J. Cell Biol.* **116**, 95-112.
- Raiborg, C., Bremnes, B., Mehlum, A., Gillooly, D. J., D'Arrigo, A., Stang, E. and Stenmark, H.** (2001). FYVE and coiled-coil domains determine the specific localisation of Hrs to early endosomes. *J. Cell Sci.* **114**, 2255-2263.
- Raiborg, C., Bache, K. G., Gillooly, D. J., Madhus, I. H., Stang, E. and Stenmark, H.** (2002). Hrs sorts ubiquitinated proteins into clathrin-coated microdomains of early endosomes. *Nat. Cell Biol.* **4**, 394-398.
- Raiborg, C., Rusten, T. E. and Stenmark, H.** (2003). Protein sorting into multivesicular endosomes. *Curr. Opin. Cell Biol.* **15**, 446-455.
- Satoh, H., Nakano, Y., Shibata, H. and Maki, M.** (2002). The penta-EF-hand domain of ALG-2 interacts with amino-terminal domains of both annexin VII and annexin XI in a Ca²⁺-dependent manner. *Biochim. Biophys. Acta.* **1600**, 61-67.
- Schmidt, M. H., Chen, B., Randazzo, L. M. and Bogler, O.** (2003). SETA/CIN85/Ruk and its binding partner AIP1 associate with diverse cytoskeletal elements, including FAKs, and modulate cell adhesion. *J. Cell Sci.* **116**, 2845-2855.
- Schmidt, M. H., Hoeller, D., Yu, J., Furnari, F. B., Cavenee, W. K., Dikic, I. and Bogler, O.** (2004). Alix/AIP1 antagonizes epidermal growth factor receptor downregulation by the Cbl-SETA/CIN85 complex. *Mol. Cell Biol.* **24**, 8981-8993.
- Schmidt, M. H., Dikic, I. and Bogler, O.** (2005). Src phosphorylation of Alix/AIP1 modulates its interaction with binding partners and antagonizes its activities. *J. Biol. Chem.* **280**, 16319-16324.
- Slot, J. W., Geuze, H. J., Gigengack, S., Lienhard, G. E. and James, D. E.** (1991). Immunolocalization of the insulin regulatable glucose transporter in brown adipose tissue of the rat. *J. Cell Biol.* **113**, 123-135.
- Strack, B., Calistri, A., Craig, S., Popova, E. and Gottlinger, H. G.** (2003). AIP1/ALIX is a binding partner for HIV-1 p6 and ELAV p9 functioning in virus budding. *Cell* **114**, 689-699.
- Vito, P., Pellegrini, L., Guet, C. and D'Adamo, L.** (1999). Cloning of AIP1, a novel protein that associates with the apoptosis-linked gene ALG-2 in a Ca²⁺-dependent reaction. *J. Biol. Chem.* **274**, 1533-1540.
- von Schwedler, U. K., Stuchell, M., Muller, B., Ward, D. M., Chung, H. Y., Morita, E., Wang, H. E., Davis, T., He, G. P., Cimbora, D. M. et al.** (2003). The protein network of HIV budding. *Cell* **114**, 701-713.
- Weed, S. A. and Parsons, J. T.** (2001). Cortactin: coupling membrane dynamics to cortical actin assembly. *Oncogene* **20**, 6418-6434.
- Wubbolts, R., Leckie, R. S., Veenhuizen, P. T., Schwarzmann, G., Mobius, W., Hoernschmeyer, J., Slot, J. W., Geuze, H. J. and Stoorvogel, W.** (2003). Proteomic and biochemical analyses of human B cell-derived exosomes. Potential implications for their function and multivesicular body formation. *J. Biol. Chem.* **278**, 10963-10972.
- Zobiack, N., Rescher, U., Ludwig, C., Zeuschner, D. and Gerke, V.** (2003). The annexin 2/S100A10 complex controls the distribution of transferrin receptor-containing recycling endosomes. *Mol. Biol. Cell* **14**, 4896-4908.